Available online at www.sciencedirect.com

ScienceDirect

Procedia CIRP 123 (2024) 446–451

www.elsevier.com/locate/procedia

7th CIRP Conference on Surface Integrity

Investigating the variation of particle distribution and surface texture of top surfaces based on build position in laser powder bed fusion

Cindy Sithole[a]*, Helia Hooshmand[b], Luke Todhunter[b], Adam Thompson[b], Sipke Hoekstra[a], Athena Jalalian[a], Samanta Piano[b], Ian Gibson[a]

[a]*Department of Design, Production and Management, Faculty of Engineering Technology, University of Twente, Drienerlolaan 5,7522 NB Enschede, The Netherlands*

[b]*Manufacturing Metrology Team, Faculty of Engineering, University of Nottingham, Nottingham, United Kingdom*

* Corresponding author. *E-mail address:* c.sithole@utwente.nl

Abstract

Quality analysis of additively manufactured (AM) surfaces is complex, yet critical for determining the functionality of parts and technology improvement. To accurately assess the quality of AM parts, it is necessary to consider the industrial application of the technology. This study investigates the variation of accumulated particles on AM top surfaces as a function of build position. It also seeks to study the surface texture variation as a function of build position, focusing on a spatial bandwidth region larger than that of traditional AM surface features, such as weld tracks, to investigate surface tension effects. Ti-6Al-4V cubes were built in a three-by-three array in a single build with fixed processing parameters. Coherence scanning interferometry was used to capture the primary data of the as-built top surfaces of cubes. The ISO 25178-2 methodology was used to extract the S-L surfaces, using the filtration methods defined in ISO 16610-21. The number of particles, coverage, and density were obtained by averaging over five repeated measurements in five different areas on the top surfaces. Particle distribution and surface texture analysis showed a trend from one location to another across the build, which is discussed according to the process variations.

Keywords: Metal Laser powder bed fusion; Quality analysis; Batch production; AM top surfaces; Surface texture; particle analysis

1. Introduction

Surface texture analysis of metal parts manufactured using laser powder bed fusion (LPBF) technology is intricate, yet critical for both product and process improvement [1]. Often, quality anomalies in LPBF technology result from processing parameters and their interactivity with the powder and energy delivery systems [2], which may lead to differences in powder density across the building substrate, gas flow turbulences, and kinematics errors in laser scanning trajectories due to speed [3]. These factors greatly influence surface texture quality and lead to spatter and partially sintered particles, the Marangoni effect, and defects on the top surface [4]. Spatter and partially sintered particles are by-products of the LPBF technology which greatly influence the surface quality of as-built additively manufactured (AM) parts. Spatter is a term used to describe material injections into the melt pool during the LPBF process due to the laser treatment zone [3,4]. Often, the spatter particles are classified by their formation during the LPBF production process. According to Ali et al., [3] and Young et al. [6], In LPBF, spatter particles can be classified as solid, which includes unmelted powder resulting from the influence of metallic vapor generated by localized laser heating on the build substrate. There are three primary types of spatter in the LPBF process: metal jet spatter (droplets), caused by vapor recoil pressure and the Marangoni effect [5]; entrainment melting

10.1016/j.procir.2024.05.078

spatter, caused by the ambient gas flow that transfers powder particles to the localised laser heating zone during production; and powder agglomeration spatter, which forms when powder and spatter agglomerate and subsequently coalesce [3]. The melting entrainment spatter may also coalesce due to increased temperature in the zone and become a droplet spatter. According to Zhang et al. [5], AM top surfaces are characterised by solid and droplet spatter caused by pressure recoil, and partially sintered particles resulting from the scanning process. Fig. 1 shows the AM top surfaces of the as-built parts with different spatter particles.

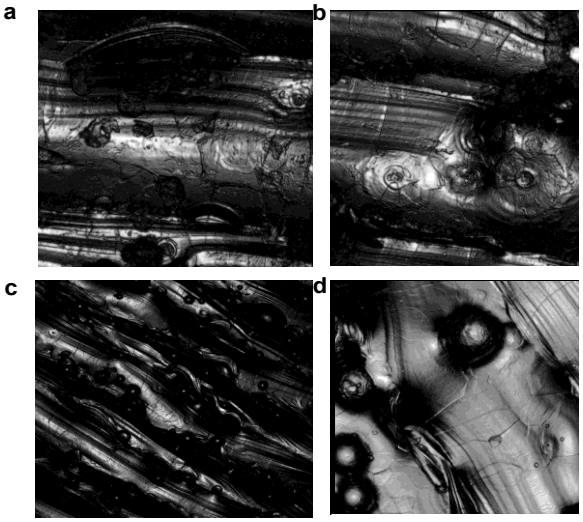

Fig. 1. (a) Solid and metal jet spatter particles on the melt track on the top surface; (b) footprints of liquid spatter on the scan track demonstrated by the circle features on the top surface; (c) a typical as-built top surface, with both liquid and solid spatter particles distributed along the scan tracks; (d) solid and powder agglomeration spatter captured on the scan track.

The trajectories of spatter particles in LPBF technology are influenced by gas flow and scan speed. As the gas flow speed increases, the spatter particle displacement also increases, leading to evenly distributed spatter particles in the direction of the gas flow and/or scan speed within a batch [7, 8]. Spatter particles can contaminate the powder bed and, in some cases, fall into the melt pool, impacting the formation of metallurgical defects, such as porosity (including lack of fusion, surface pores, and cracks) [9]. These metallurgical defects, in turn, affect the mechanical properties of the parts, leading to rejection. Hence, in-depth comprehension of the LPBF process is critical for part quality. The industrial use of LPBF technology is primarily based on the production of numerous parts within a batch. This requires a comprehensive understanding of how to produce multiple products with minimal defects and uniform quality. Subsequently, research efforts should focus on the industrial application of LPBF technology, which should include analysis of discrepancies between parts and batches [1]. Numerous studies have been conducted to explain the phenomena related to spatter particle formation, its effects, and the influence of processing parameters on surface topography and overall quality [10]. Others have explored the effects of particle size distribution and shape on surface quality [11]. Gunenthiram et al. [9] used a high-speed camera to study the displacement and velocity of spatter particles based on particle size distribution at different laser powers for materials like Ti64AlV4 and 316L steel. These studies and the broader LPBF literature indicate that process irregularities such as spatter and partially sintered particles on AM surfaces are characteristic of the LPBF process. A full understanding of these anomalies and their impact on both single and multiple parts can assist to develop a holistic quality strategy to enhance the quality of AM products.AM surface features such as scan tracks and spatter particles constitute short-scale spatial frequency commonly known as roughness while large-scale spatial frequency defines waviness [12]. Waviness in AM surfaces is due to melt-pool instability under the influence of compression and tension forces that result from the fast cooling and heating nature of the technology [3]. It is important to note that the recoil pressure is inversely proportional to the surface tension of the melt-pool surface. However, both of these factors change along the laser path, and this change is influenced by the temperature (i.e. laser power) during production. A study by Simson D & Subbu SK [10], found that waviness in the AM top surface for a single track increases with an increase in the scanning speed for a single weld track. In this study, we examine the distribution of spatter particle accumulation on the top surfaces of as-built bulk cubes as a function of build position. We also aim to study the distribution of the variation of the surface texture as a function of build position under the influence of recoater motion and gas flow direction, focusing on spatial bandwidth regions larger than that of AM top surface features, such as weld tracks and spatter particles, to investigate surface tension effects on surface texture. The cubes were built under the same processing parameters in different locations in the build platform. Additionally, this study does not classify the spatter particles on the top surface but rather studies how the spatter particles are distributed on the top surfaces of the parts in the build and then analyses the corresponding surface texture height differences within the surface as a function of build position.

2. Material and methods

2.1. Samples

The bulk cubes used in this study were manufactured in a three-by-three array, under the same processing parameters. The parts were produced by the Additive Industries laser powder bed fusion system (MetalFab1). The MetalFab1 is a modular system equipped with two Ytterbium (Yb) fiber lasers that have different working areas, a maximum laser power of 500 W and a total build volume of (420 × 420 × 400) mm. The processing parameters are presented in Table 1. The size of the bulk cubes used in this study is (10 × 10 × 10) mm. The parts were manufactured using Ti6Al4V and the process gas was argon, flowing from front to back, at 90 ° to the recoater.

Table 1. LPBF processing parameters

Parameters	Laser power/W	Laser speed/ (mm/s)	Hatch space/ mm	Layer thickness/mm
	380	1300	0.12	0.06

After production, the powder was cleaned using argon compressed air and the parts were marked and removed from the build substrate.

2.2. Data Acquisition and Measurement

The surface topography of the top surfaces of the bulk cubes was measured using the Zygo Nexview NX2 3D coherence scanning interferometer. The Zygo Nexview NX2 has a surface topography repeatability of 0.2 nm, a maximum data scan speed of 96 µm/s, and a 150 µm vertical scan range with the precision piezo drive. Five areas were selected on the top surface and measured using 5.5× magnification. Each area (the centre and four corners) was measured five times. Autofocus was applied at the start of every measurement on the selected surface. The field of view for 5.5× is (1.56 × 1.56) mm with a spatial sampling of 1.561 µm/pixel and optical (Sparrow) resolution of 1.9 µm. The scan length ranged between 280 µm and 300 µm. The extracted surface topographies were processed for both particle accumulation and surface texture analysis.

2.3. Spatter particle analysis on AM top surfaces

To analyse the spatter particle accumulation on the top surface, the Mountains Map® V9 particle analysis module was used. The software was employed in alongside ISO standards 25178-2 [13] and 16610-2 [14] to define filters for detecting particles on areal surface topographies. The number of non-measured points for the extracted surface topographies was less than 10 %. For particle identification, a Gaussian low-pass filter (S-filter) and a Gaussian high-pass filter (L-filter), both defined in ISO 25178-2 [13] were used. Based on ISO 16610-2 and ISO52173-2 [13,14], a nesting index is a parameter number that controls the filter and the way it separates the scales or wavelengths. The nesting index defines the shape or the structuring component e.g. circle or diameter [12,15]. An S-filter of 10 µm was applied to remove micro-components related to measurement noise on the extracted surface topography. The S-filtered surface was levelled using the least square plane levelling (LSPL) to remove the form and measurement tilt. After levelling, an L-filter was applied with a nesting index of 0.02 mm on the primary surface. The nesting index for a morphology filter defines the radius of the spherical elements on the extracted areal surface [15].

In this study, we used the Gaussian filter to define the radius of the spatter particles. Given the mean diameter of the powder distribution size at 38.78 µm, the 0.02 mm nesting index was considered suitable for the Gaussian filter L-filter in spatter particle analysis. The 0.02 mm approximates the radius of the mean diameter powder size. Threshold detection was then applied to specifically detect the spatter particles that were present on the extracted filtered top surface. Buchenau et al. [16], applied different thresholding methods to identify surface features and used the circle detection threshold to identify the largest diameter of the agglomerated particles on as build surfaces.

It is important to note that there are different types of thresholding methods described in both ISO 25178 and ISO 16610, which are important for feature detection on areal surface topographies. As in this paper, we aim to detect spatter particle accumulation on the top surface of bulk cubes, the circle detection threshold method was selected. The gradient setting for particle detection was five pixels at a threshold of 8 %. The aim was to detect particles with a minimum diameter of 0.02 mm and a maximum value of 0.2 mm on the top surface. The particle size distribution from the manufacturer's powder specification was d10 = 25.39 µm, d50 = 35.84 µm and the highest was d90 = 49.93 µm. The mean powder particle size was 38.78 µm. This diameter is within the range of the raw powder size used to manufacture the parts.

2.4. Surface texture analysis

The surface texture (both the large-scale and short-scale spatial frequency) in LPBF is affected by surface tension [17]. Due to the uneven distribution of temperature on the surface of the melt pool, an uneven distribution of surface tension is created [18]. During production, the laser moves according to the scan strategy increasing the temperature in the area where the laser interacts with the powder. In this region, the surface tension is low and the recoil pressure is high influencing the metal jet spatter, and as the laser passes, the surface tension of the melt pool increases and the temperature decreases. According to Shi et al [18], the higher the temperature, the lower the surface tension. This means that a surface tension gradient is formed during production, which may lead to an uneven distribution of surface texture within the batch. The surface tension gradient coupled with the fast heating and cooling nature of the process leads to a build-up of residual stresses due to the instability of the melt pool and consequently affects the surface texture. This phenomenon also influences the process by-products. The occurrence of pressure recoil and temperature gradients leads to the formation of surface features such as valleys and adjacent peaks [19], which often affect both the short and large-scale spatial frequency. In this study, we focused on surface texture rather than surface features in large-scale spatial frequency. To appropriately analyse the surface texture of surfaces measured using optical systems, filtering is applied. Filtering becomes a fundamental technique for defining the surface texture of the measured areal surface [20]. The extracted top surface topographies were filtered according to the ISO 25178-2 standard which defines the height parameters for areal surface measurements [11]. The height parameters defined by ISO 25178-2 for the areal surface texture analysis include the root-mean-square height of the scale-limited surface (*Sq*) and the arithmetic mean height of the scale-limited surface (*Sa*). In AM, *Sa* is often used for areal surface parameter analysis [15,13, 18]. However, in this study, we focus on the root-mean-square height of the scale limited surface (*Sq*), its distribution across the build, and how it varies in different locations on the measured areas of the cube. *Sq* is a scale-limited surface parameter that measures the standard deviation of the height distribution of an areal surface topography and provides a more statistical representation results of a surface [1,14,15]. For the cubes, an S-filter of 300 µm removed the scan tracks, the spatter particles, and any other small-scale lateral components on the top surface. After

removing the small-scale lateral components, the large-scale lateral components remained and was used to understand how the surface texture was changing in different locations in the build. The LSPL was used to remove form and measurement tilt.

3. Results and discussion

The spatter particle analysis results were classified and presented based on the number of particles observed, the particle density and the percentage coverage on the top surface in each measured area. Fig. 2 shows how the particles were identified after applying the S- and L- filters explained in section 2.3, and the circle detection thresholding method on selected areas of the bulk cubes.

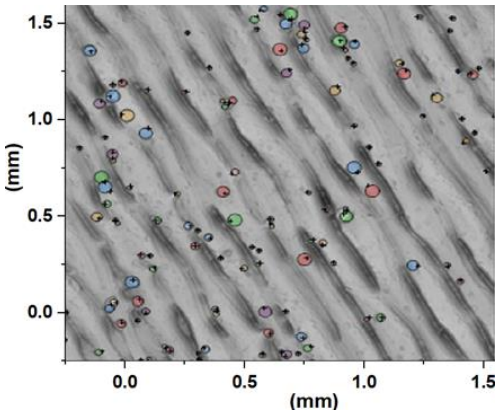

Fig. 2. (a) S-L filtered surface observed by the circle detection threshold

In Fig. 2, circle-shaped particles marked with a positive sign (+) along the scan track are observed, where the positive sign indicates the highest point of individual particles [15]. When analysing the S-L surface, different particle sizes are observed. The difference in spatter particle sizes may indicate the different types of spatter particles that are generated during the LPBF process and could be observed on AM top surfaces (Fig. 1). In this case, the enlarged particle denotes the agglomeration spatter type. While the difference in particle size is recognised, this study aims to examine the variation of spatter particle accumulation on AM top surfaces as a function of build position and their distribution across the build. The number of detected particles is affected by the filters applied. This means that changing the S-L filter nesting indices affects the number of detected particles and their density. However, it does not affect the trend or the dispersion pattern of the variation within a build.

3.1. Distribution of spatter particles on the top surface

The number of particles, density, and percent coverage in each area in a cube was averaged over the number of repeats for each measured location on top of the bulk cube. The total number of particles, particle density measures the number of particles per unit area in mm^2, and percent coverage in each cube was given by the average of all individual measurements on the top surface of the cubes. Table 2 presents the particle analysis results for each cube across the build.

Table 2. Particle analysis results per cube

Cube position	Number of spatter particles	Density of particles/ mm^2	% coverage of particles
1	58.08	23.88	1.67
2	108.96	44.80	2.94
3	106.96	42.55	2.99
4	172.52	70.93	4.39
5	178.76	73.34	4.46
6	167.56	68.90	4.72
7	132.48	54.47	3.79
8	170.40	70.06	4.84
9	63.36	26.00	2.08

The number of particles across the build range from 58.08 to 178.76, with cube 1 having the lowest particles and cube 5 having the highest number of particles on the top surface. The densities range from 23.88 to 73.34 particle/mm^2 with cube 1 having the lowest and cube 5 having the highest density. The percentage coverage ranges from 1.67 % to 4.84 %, with cube 1 being the lowest and cube 8 having the highest coverage. To analyse particle accumulation on the top surface of the bulk cubes, Fig. 3 is used to understand how the particles are distributed across the build.

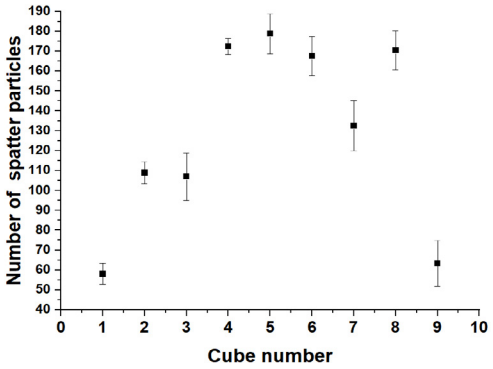

Fig. 3. Number of particle accumulation and distribution on AM top surfaces.

Fig. 3 shows the number of particles plotted as a function of build location denoted by numbers. The total standard deviation within this build is 47.2 µm with a particle accumulation mean of 128.79 µm. The particle accumulation, density, and coverage on the top surface do not follow a linear trend. The analysis took into consideration the direction of both the gas flow and the recoater position which are perpendicular to each other during production by studying the spatter particle distribution on the top surface of the cube relative to the recoater motion and gas flow direction. The process gas flow prevents metal oxidation in the chamber, channels the process by-product toward the gas flow outlet, and aids in the cooling of the metal. The shielding gas must have optimum flow speed to efficiently remove condensates without affecting the powder bed in any location in the build [21]. The particle accumulation per cube (second column in table 2) in the direction of the gas flow is analyzed from left to right using Fig. 3, starting with cube 7. The analysis of particle distribution, from cubes 7, 8, and 9 from the recoater position, exhibits a consistent pattern observed in all cubes across the build in the direction of the gas flow. This trend involves an increase from the initial position followed by a

decrease. When considering the overall distribution from the recoater position, cubes 4, 5, and 6 show an increase in particle accumulation, while cube 8 has a higher particle accumulation compared to cube 7 and cube 9 which show lower accumulation. On the other hand, cube 1 has a lower particle count when compared to cubes 2 and 3, whereas cube 2 exhibits slightly higher accumulation than cube 3. The analysis of these bulk cubes reveals that the accumulation of spatter particles on the top surface varies based on the part's location in the build, considering both the gas flow and recoater position and motion. Distinct trends emerge when comparing individual cubes to their adjacent counterparts within a build. Specifically, cubes 1, 3, 7, and 9 have the fewest particles on the top surface. Notably, the particle accumulation on the top surface is not solely attributed to gas flow and recoater factors; it appears to be influenced by a combination of processing and environmental factors during production.

3.2. Surface texture analysis based on build position

The ISO 25178 standard was applied to characterise the surface texture using the *Sq* parameter. The *Sq* height parameter corresponds to the standard deviation of heights in a scale-limited surface. The *Sq* value of the large-scale lateral components' surface height on the top surfaces of the cubes was measured by applying the filters explained in 2.4. Fig. 4 presents the surface topography of the top surface after applying the S-filter and the F-operation. The surface that remained after applying an S-filter of 300 µm and LSPL contained no spatter particles and weld tracks (Fig. 4).

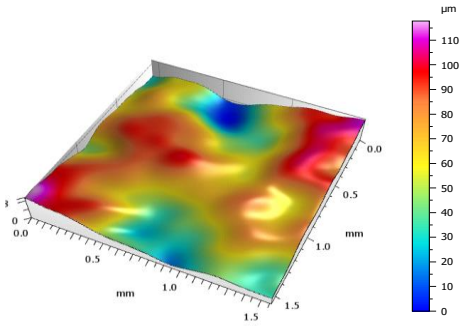

Fig. 4. S-F surface observed after applying the S-filters and F-operation.

All of these features constitute the roughness surface texture for AM top surfaces and represent process-specific characteristics of the LPBF technology. Fig. 4 shows the large-scale variation on the top surface, which can be broadly interpreted as waviness observed after removing the short-scale variation, and an even distribution of surface height is observed. In Table 3, we present the surface texture for the selected region.

Table 3.The root-mean-square (*Sq*) height per cube results

Cube position	Total *Sq* per cube/µm	Standard deviations
1	17.59	1.13
2	17.61	1.60
3	21.50	1.90
4	16.73	3.37
5	15.24	1.36
6	25.45	1.75
7	21.22	2.97
8	21.29	0.55
9	26.38	1.79

The surface texture ranges between 15 µm and 26.38 µm with a standard deviation of 3.84 µm and a surface mean of 20.34 µm. From Fig. 5, cubes 9, 6, and 3 have the highest *Sq* values when compared with the rest of the cubes. Cube 9, located at the bottom corner, has a minimal number of particles, density, and coverage; however, it has the highest *Sq* value for the large-scale variation. This behaviour could be due to the surface tension gradient that is influenced by a change in temperature and the recoil pressure as the laser moves past and the position of cube 9 (which has few adjacent parts), which could increase the surface tension leading to a difference in surface heights. This can be validated with cube 5 which is located in the centre of the build plate and has many adjacent parts, the temperature in cube 5 decreases at a steady pace, hence has an *Sq* value of 15.24 µm and the highest number of particle accumulation due to the vapor recoil pressure and scan speed (1300 mm/s^2).

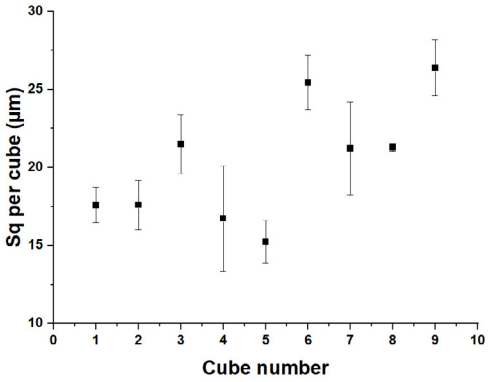

Fig 5. The distribution of *Sq* for large-scale variation analysis.

The results also indicate that the *Sq* value decreases in the direction of the gas flow. When observing the *Sq* value from the recoater position, the surface height increases from left to right for cubes 7, 8, and 9. The same trend is observed for cubes 1, 2, and 3, whereas cubes 4, 5, and 6, located in the middle of the array, seem to exhibit random variations. From the analysed results, it is evident that the *Sq* value for large-scale variation is not evenly distributed across the build substrate; instead, it varies with the position of the cube in relation to the gas flow and the recoater position. The same observation holds within each cube, as the top surface is not uniform. The surface texture due to large-scale spatial frequency was analyzed in areas with a (1.56 × 1.56) mm field of view. However, it's important to note that the analyzed areas may not be large enough to fully ascertain the effect of surface tension on large-scale variations of a surface.

4. Conclusion

In this study, we explored the accumulation of spatter particles on the top surface of AM components within a batch at different build positions under the influence of the recoater motion and gas flow direction. The study delineated the formation of spatter particles and their subsequent accumulation on the top surfaces of bulk cubes. This accumulation is influenced by the position of the recoater and the direction of the gas flow. The gas flows from the front to the back perpendicular to the recoater motion. Furthermore, the

degree of accumulation varies among the cubes based on their positions on the build substrate. While the accumulation of spatter particles can be affected by the direction of the gas flow and the recoater's position and movement,. The results also indicate a significant impact from adjacent parts within the build and environmental parameters that influence the surface tension of the melt pool and process by-products. Notably, the number of accumulated particles either increases or decreases depending on the part's location relative to the gas flow direction and recoater position, even when parts are built under the same processing parameters. Specifically, the number of accumulated particles increases for cubes positioned in the center of the build plate in relation to the gas flow direction, while cubes located on the right side exhibit a slight decrease in the same direction. Regarding the surface texture of the bulk cubes, it can be observed that the *Sq* value increases from left to right relative to the recoater position, of the bulk cubes in the middle row. The distribution of *Sq* values in the direction of the gas flow for the middle row and column appears random, as does the distribution from the recoater position for all the cubes, without following a defined trend. Understanding the accumulation of spatter particles on the AM top surface is crucial for gaining insights into potential defects that could impact the performance and functionality of the resulting products. Most importantly, the analysis and understanding of spatter particle developments could yield crucial insights about the AM production process for batch productions, serving as a building block for developing a quality strategy. Based on these findings, future work will focus on analysing the relationship between spatter particle accumulation and surface texture. This research will also encompass an investigation into the distribution of large-scale lateral components using an extended field of view. Future works will consider developing a rigorous strategy for managing variation within a batch and between batches.

Acknowledgements

This work is based on the research supported wholly by the National Research Foundation of South Africa (Grant Numbers: 120210) and the Department of Design, Production, and Management at the University of Twente. We would like to acknowledge and thank the Manufacturing Metrology Team at the University of Nottingham for their immense involvement in this work.

References

[1] Townsend A, Senin N, Blunt L, Leach RK, Taylor JS. Surface texture metrology for metal additive manufacturing: a review. Precis Eng 2016;46:34–47.

[2] King WE, Anderson AT, Ferencz RM, Hodge NE, Kamath C, Khairallah SA, et al. Laser powder bed fusion additive manufacturing of metals; physics, computational, and materials challenges. Appl Phys Rev. 2015;2(4):041304.

[3] Ali U, Esmaeilizadeh R, Ahmed F, Sarker D, Muhammad W, Keshavarzkermani A, et al. Identification and characterization of spatter particles and their effect on surface roughness, density, and mechanical response of 17-4 PH stainless steel laser powder-bed fusion parts. Mater Sci Eng. 2019;756(April):98–107.

[4] Liu C, Law ACC, Roberson D, Kong Z (James). Image analysis-based closed-loop quality control for additive manufacturing with fused filament fabrication. J Manuf Syst. 2019;51:75–86.

[5] Zhang H, Krishna C, Vallabh P, Zhao X. Influence of Spattering on In-process Layer Surface Roughness during Laser Powder Bed Fusion. (412):1–34.

[6] Young ZA, Guo Q, Parab ND, Zhao C, Qu M, Escano LI, et al. Types of spatter and their features and formation mechanisms in laser powder bed fusion additive manufacturing process. Addit Manuf. 2020;36:101438.

[7] Ahmed Obeidi M, Mussatto A, Groarke R, Vijayaraghavan RK, Conway A, Rossi Kaschel F, et al. Comprehensive assessment of spatter material generated during selective laser melting of stainless steel. Mater Today Commun. 2020;25:101294.

[8] Esmaeilizadeh R, Ali U, Keshavarzkermani A, Mahmoodkhani Y, Marzbanrad E, Toyserkani E. On the effect of spatter particle distribution on the quality of Hastelloy X parts made by laser powder-bed fusion additive manufacturing. J Manuf Process. 2019;37:11–20.

[9] Gunenthiram V, Peyre P, Schneider M, Dal M, Coste F, Gunenthiram V, et al. Experimental analysis of spatter generation and melt-pool behavior during the powder bed laser beam melting process: HAL Id : hal-01825515. J Mater Process Tech. 2018;251:376–86.

[10] Simson D, Subbu SK. Effect of Process Parameters on Surface Integrity of LPBF Ti6Al4V. Procedia CIRP. 2022;108(C):716–21.

[11] Sendino S, Martinez S, Lartategui F, Gardon M, Lamikiz A, Gonzalez JJ. Effect of powder particle size distribution on the surface finish of components manufactured by laser powder bed fusion. Int J Adv Manuf Technol. 2023;124(3–4):789–99.

[12] Leach R, Leigh Brown XJ, Blunt R, Mike Conroy DM. Guide for the Measurement of Smooth Surface Topography using Coherence Scanning Interferometry. In: Manual. 2008. p. 56.

[13] ISO 25178-2. Geometrical product specifications (GPS) — Surface texture: Areal — Part 2: Terms, definitions, and surface texture parameters. International Organization for Standardization 2012 p. 54.

[14] ISO 16610-2. Geometrical product specifications (GPS): surface texture: areal: part 3: specification operators. Eur Comm Stand. 2023;62.

[15] Digital surf, MountainsMapreference manual: Surface Imaging and Metrology Software. Frace: Digital surf, 2015

[16] Buchenau T, Thompson A, Brüning H, Amkreutz M, Mayer B. Surface Features of As-built Metal Additive AlSi7Mg0 . 6. 2023:0–5.

[17] Khorasani M, Ghasemi A, Awan US, Hadavi E, Leary M, Leary M, et al. A study on surface morphology and tension in laser powder bed fusion of Ti-6Al-4V. Int J Adv Manuf Technol. 2020;(111):2891–909.

[18] Shi Y, Yan C, Zhou Y, Wu J, Wang Y, Yu S, et al. Metal materials for additive manufacturing. In: Materials for Additive Manufacturing. Elsevier; 2021. p. 403–595.

[19] Samadian K, de Waele W. Fatigue crack growth model incorporating surface waviness for wire+arc additively manufactured components. Procedia Struct Integr . 2020;28:1846–55

[20] Thompson A, Newton L, Leach R. New Standard for Metal Powder Bed Fusion Surface Texture Measurement and Characterisation. Metrology. 2023;3(2):237–45.

[21] Chen Z, Wu X, Davies CHJ (2021) Process variation in Laser Powder Bed Fusion of Ti-6Al-4V. 41: